Superlattices and Microstructures 120 (2018) 402–409

Contents lists available at ScienceDirect

Superlattices and Microstructures

journal homepage: www.elsevier.com/locate/superlattices

Photoelectrical properties of fabricated ZnS/Si heterojunction device using thermionic vacuum arc method

H.K. Kaplan, S.K. Akay*, M. Ahmetoglu

Department of Physics, Faculty of Sciences and Arts, Uludag University, 16059 Görükle, Bursa, Turkey

ARTICLE INFO

Keywords:
ZnS/Si
Heterojunction
Photoelectrical
Photoluminescence
TVA

ABSTRACT

ZnS thin films have been successfully deposited with the same production parameters using thermionic vacuum arc technique on glass and silicon substrates. UV–Vis absorbance spectra and photoluminescence measurements were performed for the optical characterization of ZnS/glass thin film and ZnS/p-Si heterojunction device, respectively. The optical band gap is found approximately 3.78 eV. Further, electrical parameters of the device were determined for the current-voltage (I-V) measurements in dark and under illumination conditions. The open-circuit voltage and the short-circuit current values have been obtained related to illumination I-V measurements. Also, we have utilized photocurrent measurements to investigate the wavelength dependent to photosensitivity of the ZnS/p-Si heterojunction device.

1. Introduction

In recent years, ZnS thin films have attracted a great deal of attention due to the highest wide band gap value among the binary semiconductors and their excellent luminescent properties from ultraviolet to near infrared. With these features, they have been involved as a host material in the fabrication of optoelectronic devices such as PV cells, photodetectors, etc. [1–3].

Many studies have been carried out to produce ZnS thin films on Si, GaAs or glass substrates in various fields using RF sputtering [4], metal organic vapor-phase epitaxy [5], chemical bath deposition [6], pulsed laser deposition [7] and molecular beam epitaxy (MBE) [8]. As an alternative to these methods, Thermionic vacuum arc (TVA) technique [9] has been preferred due to the short processing time, high deposition rate and a low production cost of the thin films such as ZnS, AlGaN and GaN.

As stated by Bouguila et al. [10], there is not much research about the photoresponse properties of ZnS/Si heterojunction structures in literature. They said, in their work, that the heterojunction structure fabricated by spray technique showed photovoltaic effect but, in consequence of low and weak photovoltaic properties, such structures should be improved.

In this paper, we focused on the photoresponse properties of ZnS/Si heterojunction device fabricated using thermionic vacuum arc technique. Besides, current-voltage (I-V) characteristics in dark and illumination was obtained to investigate electronic properties of the heterojunction device.

2. Experimental procedure

ZnS thin films were deposited on well-cleaned glass and p-type Si (1–10 Ω cm resistivity and (100) orientation) substrates for obtaining ZnS/p-Si heterojunction device under such circumstances. After the standard cleaning procedure [11], except glass substrate, the unpolished surface of p-type Si substrate made ohmic contact (Al) by using thermal evaporation in a vacuum coating unit

* Corresponding author.
E-mail address: kakay@uludag.edu.tr (S.K. Akay).

https://doi.org/10.1016/j.spmi.2018.05.055
Received 8 March 2018; Received in revised form 24 May 2018; Accepted 24 May 2018
Available online 26 May 2018
0749-6036/ © 2018 Elsevier Ltd. All rights reserved.

of 1×10^{-5} Torr. The thickness of ohmic contact was around 100 nm. Then, Si substrate was heated at 400 °C for 10 min in the N_2 atmosphere to form good ohmic contacts. The substrates were placed at a distance of 7 cm above the target. A granule ZnS (Alfa Aesar's), 6 mm in size, consisting of 99.995% purity was used as a target and during the deposition, the chamber vacuum was kept at 7×10^{-5} Torr. The filament current applied to the cathode was 18 A. Applied voltage between anode and cathode and discharge current was 0.3 A and 200 V, respectively. The generated plasma occurred around the electrodes and the deposition process continued for 4 min. The elemental and surface analysis of ZnS thin film were carried out by EDX (Bruker AXS Microanalysis) and AFM (Nanomagnetics Instruments).

The optical transmittance of the ZnS thin film grown on the glass substrate was determined by Unico SQ4802 UV/vis spectrophotometer in 200–1100 nm wavelength range at room temperature to obtain the band gap of ZnS thin film. The refractive index of ZnS thin film was performed by FilMetrics F20 Thin Film Analyzer. Photoluminescence (PL) spectra of the ZnS/Si heterojunction dependent on the temperature were performed by 325 nm He-Cd laser with output power density of 200 mW (Dongwoo Optron). Measurements were taken at different temperatures ranging from 10 K to 300 K using He closed cryostat. A Czerny-Turner type monochromator system fitted with the Hamamatsu PMT detector was utilized for signal detection. The current-voltage (I-V) measurements of fabricated Al/p-Si/n-ZnS/Al heterojunction device in dark and illumination were performed by means of Keithley 2440 5 A sourcemeter and Oriel 1000 W solar cell simulator setup (under AM 1.5G conditions), respectively.

Photo response spectra of the Al/p-Si/n-ZnS/Al heterojunction device were measured in the range of 860–1160 nm with a setup of Oriel Apex2 100 W quartz tungsten halogen lamb, Cornerstone 260 monochromator and SR830 DSP Lock-In-Amplifier. The sensitivity of investigated samples were estimated with Thorlabs PDA200C photodiode amplifier. Spectral photocurrent measurement in the range of 250–800 nm was performed with a setup of Thermo Oriel Xenon lamp, Jobin Yvon Triax 550 monochromator and Keithley 1657a electrometer.

3. Results and discussion

The elemental composition of Zn and S in ZnS thin film was observed as 52% Zn and 48% S with EDX analysis. The surface structure and surface roughness value of the ZnS thin film was defined by AFM analysis. As seen in Fig. 1, the ZnS thin film surface is uniform. The surface roughness value and average grain size were found to be 2 nm and 31 nm, respectively. As stated by Nayef [12], if the surface is uniform and the surface roughness value is lower, the light reflection is reduced and more light can be absorbed by the surface.

Optical transmission spectra of ZnS thin film grown on a glass substrate is shown in Fig. 2. The average transmittance value in the visible region was realized just under 90%. This high transmittance value demonstrates that the fabricated film has highly crystalline structure [13]. To calculate optical band gap (E_g) of the ZnS thin film Tauc's equation can be used [14].

$$\alpha h\nu = A(h\nu - E_g)^m \tag{1}$$

Here, m equal to ½, A, h, α and hν are the constant, Planck's constant, absorption coefficient and the photon energy, respectively.

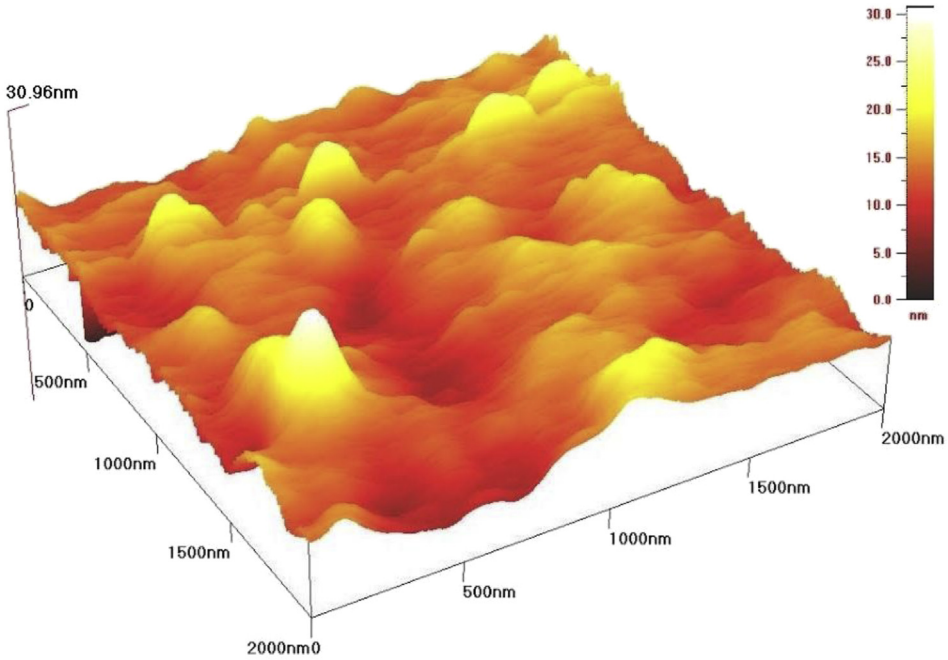


Fig. 1. AFM image ($2 \times 2\,\mu m^2$) of ZnS thin film grown on p-Si substrate.

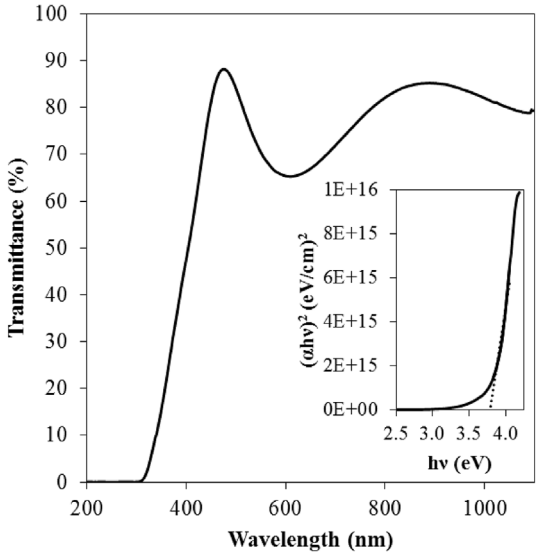


Fig. 2. The plot of transmittance vs. wavelength for ZnS thin film. The inset shows $(\alpha h\nu)^2$ vs. hν plot.

As seen in the inset of Fig. 2 which shows the plot of $(\alpha h\nu)^2$ vs. hν for ZnS thin film, the optical band gap of ZnS thin film is estimated to be 3.78 eV. By using transmittance data of ZnS thin film, the refractive index values were calculated with the Swanepoel equation [15].

$$n(\lambda) = \left[\left(\frac{2s(T_{Max}(\lambda) - T_{min}(\lambda)}{T_{Max}(\lambda)T_{min}(\lambda)} + \frac{s^2+1}{2} \right) + \sqrt{\left(\left(\frac{2s(T_{Max}(\lambda) - T_{min}(\lambda)}{T_{Max}(\lambda)T_{min}(\lambda)} + \frac{s^2+1}{2} \right)^2 - s^2 \right)} \right]^{1/2} \quad (2)$$

Here, T_{max} (λ) is the transmittance maxima, T_{min} (λ) is the transmittance minima, s is refractive index value of the substrate and n(λ) is the refractive index, respectively. Obtained results from the Swanepoel equation were compared with the FilMetrics results. Both measurement results are in concordance with each other (Table 1). Fig. 3 shows refractive index (n) versus wavelength dependency for ZnS thin film grown on a glass substrate. It can be seen in Fig. 3 that the refractive index decreases with increasing wavelength. It changes from 2.68 to 2.36. This variation coincides with literature [12,16].

Fig. 4 illustrates the temperature-dependent PL spectra of the ZnS/Si heterojunction device. It is seen in Fig. 4 that the luminescence intensity increases with decreasing temperature. The temperature-dependent PL spectra shows three separate peaks located at 328 nm, 395 nm and 520 nm. These peaks are corresponded at energies of 3.78 eV, 3.14 eV and 2.38 eV, respectively. The peak located at 328 nm is known as near band-edge (NBE) PL emission, while the emission peak at 395 nm can be referred to as the ultraviolet luminescence (UVL) band. Abounadi et al. [17] observed two emission peaks at 326.46 nm and 326.2 nm in the PL measurements of ZnS epilayers grown by the metal organic chemical vapor deposition method on Si substrate. They expressed that the first one was corresponded to the light-hole exciton, while the second one was regarded to the heavy-hole exciton. Mizuhata et al. [18] stated that the emission peak observed at around 520 nm was related to the transition from ZnS/PSi interface level, whereas Sanz et al. [19] pointed out that the peak at 520 nm was relative to the electron transition between the energy levels of the Sulfur and Zinc vacancies and this was interrelated to the composition of the material. Along with the contributions of the authors, in our study, we concluded that the emission peak in which position was wide and spread observed at the level of defect transition was related to structural defects. Besides, this emission peak corresponds to green luminescence.

Fig. 5a–c shows that the PL intensity corresponding to three different peaks is plotted as a function of 1000/T. Fig. 5a and c shows that PL intensity is increased with a decreasing temperature of 300 to 50 K, but in Fig. 5b, the PL intensity in this temperature region shows irregularity. When the temperature reaches to 250 K, the PL intensity decreases monotonically (150 K) and then it increases to 50 K. As can be seen in Fig. 5a–c, PL intensities increase at all three emission peaks beyond 50 K.

Band gap diagram of n-ZnS/p-Si heterojunction device is shown in Fig. 6. For p-Si, the band gap (Eg_2) and electron affinity (χ_p) were regarded as 1.12 eV and 4.01 eV, while the bandgap (Eg_1) and electron affinity (χ_n) of n-ZnS were 3.78 eV and 3.9 eV,

Table 1
Comparative refractive index values.

λ(nm)	n(λ) Swanepoel	n(λ) FilMetrics
476	2.57	2.52
610	2.46	2.43
890	2.40	2.37

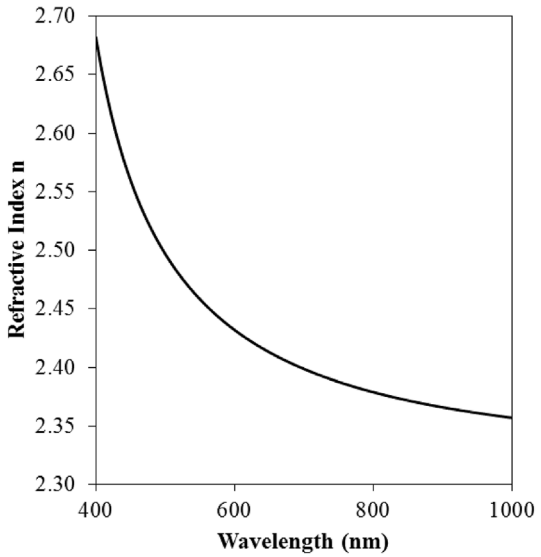


Fig. 3. Refractive index vs. wavelength dependency for produced ZnS thin film.

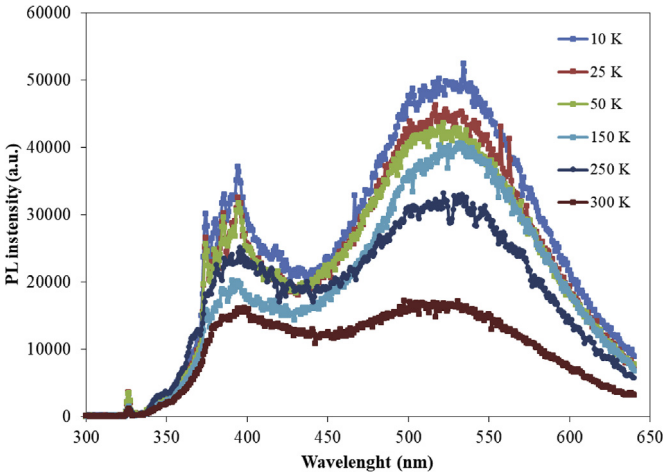


Fig. 4. Temperature dependent photoluminescence spectra of ZnS/p-Si heterojunction device from 10 to 300 K.

respectively [20]. As observed in Fig. 6, it is stated that the electron diffusion from *p*-Si to n-ZnS and a hole diffusion from n-ZnS to p-Si from p-n heterojunction is realized.

I-V measurements of Al/p-Si/n-ZnS/Al heterojunction device in dark and illumination at 300 K are shown in Fig. 7. In both cases, the device shows rectifying behavior. This behavior verifies p-n heterojunction between ZnS and p-Si. Furthermore, under illumination, I-V measurements show that ZnS/Si heterojunction device has light sensitivity. In addition to this, ideality factor (n) and barrier height (Φ_b) were determined in dark and illumination at 300 K. In dark, n and Φ_b were measured as 2.72 and 0.72 eV, while under illumination these parameters were found to be 2.34 and 0.68, respectively. According to literature, in dark condition n value is consistent with Huang et al. [21]. These measurement results were calculated by standard diode expression [22].

From I-V measurements in illumination, we have obtained open-circuit voltage and short-circuit current values as $V_{oc} = 100$ mV and $I_{sc} = 8.11 \times 10^{-5}$ mA, respectively. These values are slightly higher in comparison with Bouguila et al. [10], but it still needs to be improved to be considered as a solar cell.

The spectral distribution of the sensitivity of the ZnS/Si heterojunction device at two different temperatures is shown in Fig. 8. By using the shift from the long wavelength side of the photoresponse, we have estimated the temperature coefficient of the gap width of Si layer.

The temperature coefficient of the band gap of Si layer was found to be $\Delta E_g/\Delta T = 3 \times 10^{-4}$ eV/K. This value is consistent with the temperature coefficient obtained from the temperature dependence of the band gap of Si [23].

$$E_g = 1.17 - 4.73 \times 10^{-4} \frac{T^2}{T + 636} (eV) \tag{3}$$

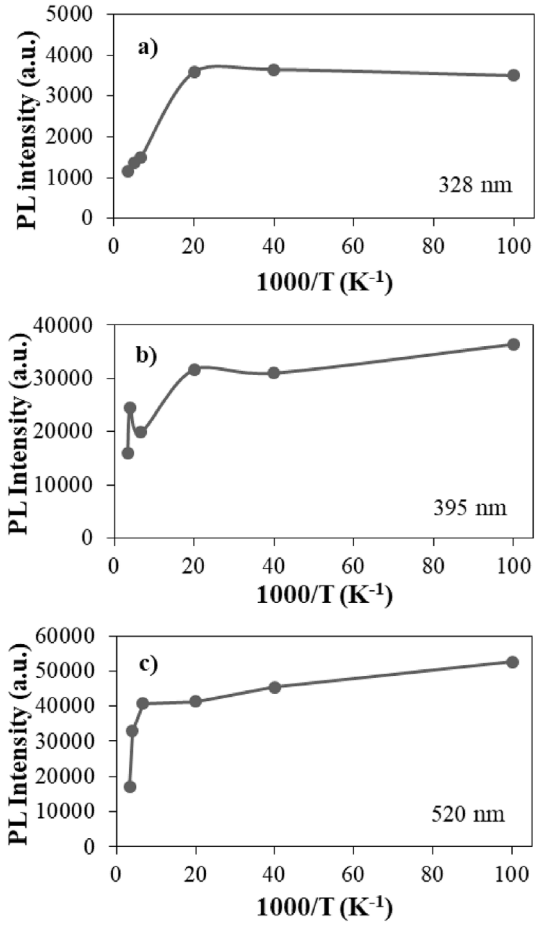


Fig. 5. The PL intensity variation with temperature a) 328 nm, b) 395 nm and c) 520 nm.

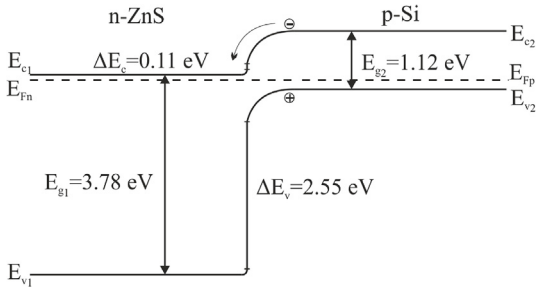


Fig. 6. Energy band diagram of n-ZnS/p-Si heterojunction in equilibrium.

Si band gap determined from the wavelength corresponding to a two times decrease in sensitivity [24,25] is 1.07 ± 0.02 eV at 300 K. This value is consistent with the Si band gap at 300 K.

From the room temperature spectral photocurrent measurement which covers the UV region of the EM spectrum, we have obtained results that the device has a relatively high increasing response to decreasing wavelengths from 460 nm. The measurement data is given in Fig. 9. This data indicates that the device has potential for UV photo-detector applications.

The photocurrent (I_{ph}) depends on the excess energy which is equal to the difference between the photon energy ($h\nu$) and the band gap (E_g). From the semiconductor band gap edge, the proportion of the photocurrent in relation to the excess energy determines the type of the band gap. The band gap was calculated from the above equation [26,27].

Direct Bandgap:

$$I \propto (h\nu - E_g)^2 \tag{4}$$

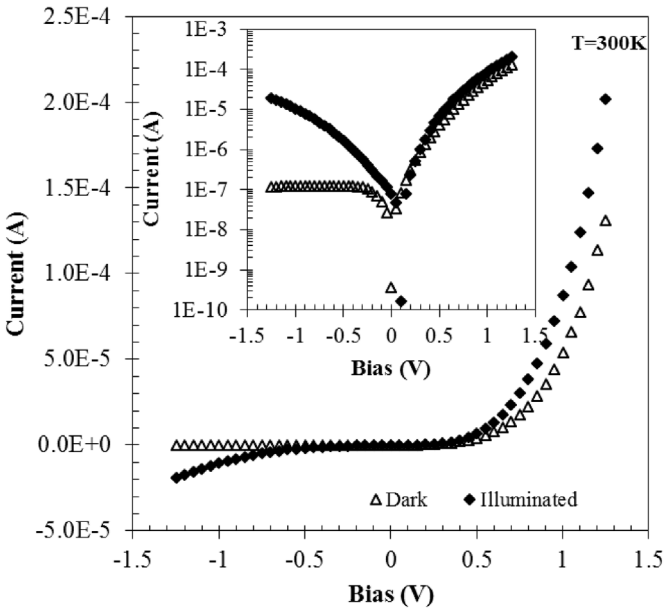


Fig. 7. I-V plots of ZnS/p-Si heterojunction device in dark and illumination (under 1 Sun) at 300 K. The inset shows semi-log current vs. voltage characteristics of the same measurement results.

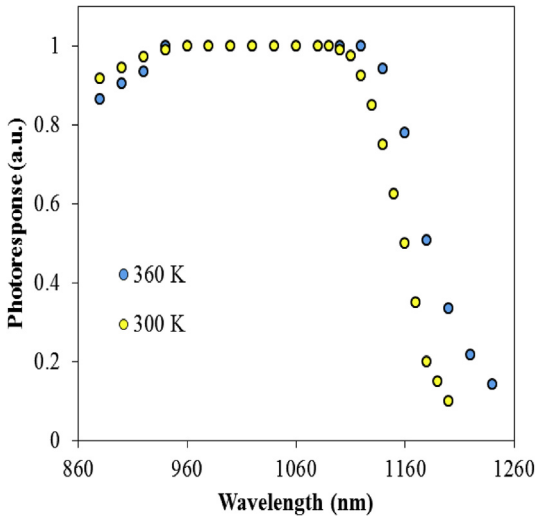


Fig. 8. The spectral distribution of sensitivity for a ZnS/Si heterojunction device at two different temperatures.

$$I^2 \propto (h\nu - E_g) \tag{5}$$

Indirect Bandgap:

$$I \propto (h\nu - E_g)^2 \tag{6}$$

According to Eq. (6) as a function of the photon energy, photocurrent values near the cut-off of 458 nm are shown in Fig. 10. With this figure, it is possible to determine the Si band gap. The point where the line cuts the x-axis gives Si band gap and it is found to be about 1.01 ± 0.02 eV.

4. Conclusion

ZnS nanofilms were successfully grown by TVA technique on a glass substrate and p-Si to form p-n heterojunction device. It has been found that the fabricated device exhibits p-n characteristics both in dark and illumination conditions at 300 K. The PL measurements performed at different temperatures of ZnS thin film grown on p-Si substrate show three peaks located at 328 nm, 395 nm and 520 nm. The green emission peak at 520 nm is broad and it indicates that the emission is related to the structural defects. The

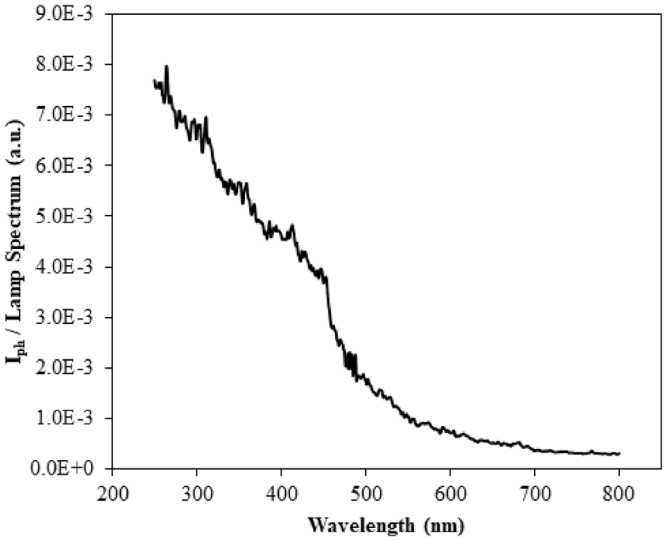


Fig. 9. I_{ph}/Lamp spectrum vs. wavelength of the ZnS/Si heterojunction device.

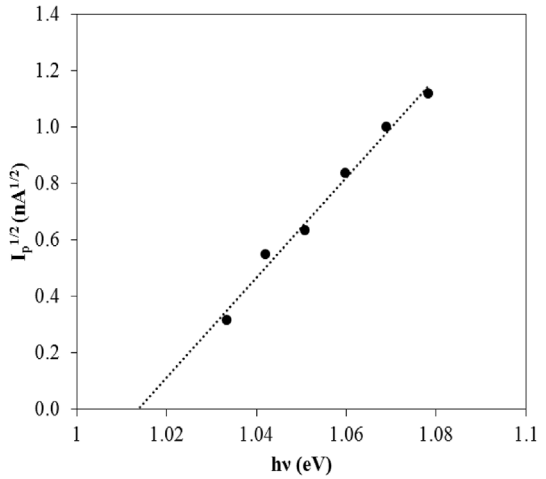


Fig. 10. The plot of the root of photocurrent versus photon energy near the band edge.

fabricated p-n heterojunction device is sensitive to the light in the range of 860–1160 nm, also the device has an increasing response to decreasing wavelengths from 460 nm. Photocurrent measurements show that ZnS/p-Si heterojunction device can be used as a UV photo-detector, while the photo sensitivity measurement indicates that the device has also potential of photo-detector for wavelengths between 860 nm and 1160 nm.

Appendix A. Supplementary data

Supplementary data related to this article can be found at http://dx.doi.org/10.1016/j.spmi.2018.05.055.

References

[1] K. Nagamani, N. Revathi, P. Prathap, Y. Lingappa, K.T. Ramakrishna Reddy, Al-doped ZnS layers synthesized by solution growth method, Curr. Appl. Phys. 12 (2012) 380–384.
[2] J. Díaz-Reyes, R. Castillo-Ojeda, J. Martínez-Juárez, O. Zaca-Moran, J.E. Flores-Mena, M. Galván-Arellano, Growth and characterization of ZnS nano films grown by RF magnetron sputtering on GaAs, Int. J. Cir. Sys. Sig. Process. 8 (2014) 15–21.
[3] C.F. Wang, B. Hub, W.B. Li, H.H. Yi, Luminescence properties of ZnS/porous Si composites, Optik 125 (2014) 554–556.
[4] V.L. Gayou, B. Salazar-Hernandez, M.E. Constantino, E. Rosendo Andrés, T. Diáz, R. Delgado Macuil, M. Rojas López, Structural studies of ZnS thin films grown on GaAs by RF magnetron sputtering, Vacuum 84 (2010) 1191–1194.
[5] O. Briot, N. Briot, A. Abounadi, B. Gil, T. Cloitre, R.L. Aulombard, Reflectivity analysis of ZnS layers grown on GaAs and Si substrates by metalorganic vapour-phase epitaxy, Semicond. Sci. Technol. 9 (1994) 207–209.
[6] M. Rosado-Mendoza, A.I. Oliva, Chemical bath deposition of Zinc Sulfide films doped with copper, Mater. Manuf. Process. 31 (2016) 1454–1460.

[7] W. Zhang, X. Zeng, J. Lu, H. Chen, Phase controlled synthesis and optical properties of ZnS thin films by pulsed laser deposition, Mater. Res. Bull. 48 (2013) 3843–3846.
[8] M.M. Islam, S. Ishizuka, A. Yamada, K. Sakurai, S. Niki, T. Sakura, K. Akimoto, CIGS solar cell with MBE-grown ZnS buffer layer, Sol. Energy Mater. Sol. Cells 93 (2009) 970–972.
[9] M. Özkan, N. Ekem, S. Pat, M.Z. Balbağ, ZnS thin film deposition on Silicon and glass substrates by Thermionic Vacuum Arc, Mater. Sci. Semicond. Process. 15 (2012) 113–119.
[10] N. Bouguila, D. Bchiri, M. Kraini, A. Timoumi, I. Halidou, K. Khirouni, S. Alaya, Structural, morphological and optical properties of annealed ZnS thin films deposited by spray technique, J. Mater. Sci. Mater. Electron. 26 (2015) 9845–9852.
[11] H.K. Kaplan, S. Sarsıcı, S.K. Akay, M. Ahmetoglu, The characteristics of ZnS/Si heterojunction diode fabricated by thermionic vacuum arc, J. Alloy. Comp. 724 (2017) 543–548.
[12] U.M. Nayef, Improve the efficiency of UV-detector by modifying the Si and porous silicon substrate with ZnS thin films, Optik 130 (2017) 441–447.
[13] D.H. Hwang, J.H. Ahn, K.N. Hui, K.S. Hui, Y.G. Son, Structural and optical properties of ZnS thin films deposited by RF magnetron sputtering, Nanoscale Res. Lett. 7 (2012) 26.
[14] J.C. Tauc, Optical Properties of Solid, North-Holland, Amsterdam, 1972, p. 372.
[15] R.J. Swanepoel, Applications and processing of transparent conducting oxides, J. Phys. E Sci. Instrum. 16 (1980) 1214.
[16] O. Özakın, B. Güzeldir, M.A. Yıldırım, M. Sağlam, A. Ateş, Influence of film thickness on structural and optical properties of ZnS thin films obtained by SILAR method and analysis of Zn/ZnS/n-GaAs/In sandwich structure, Phys. Status Solidi A 209 (2012) 687–693.
[17] A. Abounadi, M. Di Blasio, D. Bouchara, J. Calas, M. Averous, O. Briot, N. Briot, T. Cloitre, R.L. Aulombard, B. Gil, Reflectivity and photoluminescence measurements in ZnS epilayers grown by metal-organic chemical-vapor deposition, Phys. Rev. B 50 (16) (1994) 11677–11683.
[18] M. Mizuhata, Y. Mineyama, H. Maki, Fabrication of ZnS/Porous Silicon composite and its enhancement of photoluminescence, Electrochim. Acta 201 (2016) 86–95.
[19] M. Sanz, M.L. Arias, R. de Nalda, S. Amoruso, G. Ausanio, S. Lettieri, R. Bruzzese, X. Wang, M. Castillejo, Ultrafast laser ablation and deposition of wide band gap semiconductors, J. Phys. Chem. C 115 (2011) 3203–3211.
[20] I. Tapan, M.A. Ahmetoglu (Afrailov), F. Kocak, A ZnS–Si isotype heterojunction avalanche photodiode structure for scintillation light detection, Nucl. Instrum. Meth. 567 (2006) 268–271.
[21] J. Huang, L.J. Wang, K. Tang, R. Xu, J.J. Zhang, X.G. Lu, Y.B. Xia, Photoresponse properties of an n-ZnS/p-Si heterojunction, Chin. Phys. Lett. 28 (2011) 127301.
[22] S.M. Sze, Physics of Semiconductor Devices, second ed., John Wiley & Sons, New York, 1981.
[23] M. Levinshtein, M. Shur, S. Rumyantsev, Handbook Series on Semiconductor Parameters vol. 1, Word Scientific, 1996, p. 3.
[24] M.A. Afrailov, Photoelectrical chracteristics of the InAsSbP based uncooled photodiodes for the spectral range 1.6-3.5μm, Infrared Phys. Technol. 53 (2010) 29–32.
[25] M. Ahmetoglu (Afrailov), B. Kucur, I.A. Andreev, E.V. Kunitsyna, M.P. Mikhailova, Yu P. Yakovlev, Electrical and optical properties of the GaInAsSb-based heterojunctions for infrared photodiode and thermophotovoltaic cell application, Infrared Phys. Technol. 53 (2010) 399–403.
[26] X. Mathew, Does the band gap calculated from the photocurrent of Schottky devices leads to erroneous results? Analysis for CdTe, J. Phys. D Appl. Phys. 33 (2000) 1565–1571.
[27] E. Coşkun, H.H. Güllü, İ. Candan, Ö. Bayraklı, M. Parlak, Ç. Erçelebi, Device behavior of an In/p-Ag(Ga, In)Te2/n-Si/Ag Heterojunction diode, Mater. Sci. Semicond. Process. 34 (2015) 138–145.